Probing the nucleon structure with SIDIS at Jefferson Lab.

Sergio Anefalos Pereira[1,]

INFN Frascati

Via Enrico Fermi, 40 Frascati (RM) Italy CAP 00044

Abstract

In recent years, measurements of azimuthal moments of polarized hadronic cross sections in hard processes have emerged as a powerful tool to probe nucleon structure. Many experiments worldwide are currently trying to pin down various effects related to nucleon structure through Semi-Inclusive Deep-Inelastic Scattering (SIDIS). Azimuthal distributions of final-state particles in SIDIS, in particular, are sensitive to the orbital motion of quarks and play an important role in the study of Transverse Momentum Dependent parton distribution functions (TMDs). The CLAS spectrometer, installed in Hall-B at Jefferson Lab, has collected semi-inclusive data using the CEBAF 6 GeV polarized electron beam on polarized solid NH_3 and ND_3 targets. An overview of these measurements is presented.

Keywords:

1. Introduction

Describing the complex structure of the nucleon in terms of the partonic degrees of freedom of QCD has been one of the main goals of subatomic physics research. Our knowledge of the universal parton distribution functions (PDFs) and the fragmentation functions (FFs), that connect the partonic dynamics to the observed hadrons has been improved in recent years. As a probability density to find a parton (quark or gluon) inside a hadron carrying a fraction x of the hadron's longitudinal momentum, the PDFs have provided us information about the partonic structure of a hadron. The partonic structure of hadrons has been investigated beyond the PDFs by exploring the parton's motion and spatial distribution perpendicular to the momentum transfered to the hadron.

TMDs are studied at JLab through SIDIS on nucleons (and nuclei) with various experimental equipment. Measuring transverse momentum of final-state hadrons in SIDIS gives access to the transverse momentum distributions (TMDs) of partons, and spin asymmetries measurements give us access to several TMDs, providing information on how quarks are confined in hadrons. Here we will concentrate on CLAS detector using a linearly polarized target.

2. Jefferson Lab and the CLAS detector

The CEBAF (Continuous Electron Beam Accelerator Facility) accelerator at Jefferson Lab is capable of delivering electrons with an energy range of 0.8-6.0 GeV, a maximum current of 200μA and beam polarizations of $\sim$ 85%. It can simultaneously deliver beams to 3 halls. The CLAS (CEBAF Large Acceptance Spectrometer) [1] utilizes a non-uniform toroidal magnetic field generated by six superconducting coils which define six independent modules.

The targets can be longitudinally and transversely polarized with respect to the incident beam. The large acceptance, coupled with a luminosity of $10^{34}\ cm^{-2}s^{-1}$, allows precise asymmetry measurements over a broad kinematical range.

3. Results

3.1. Double-Spin Asymmetry

The double-spin asymmetry, A_1, is defined as

$$A_1 = \frac{1}{fD'(y)P_bP_t}\frac{N^+ - N^-}{N^+ + N^-} \propto \frac{g_1(x,P_T)}{f_1(x,P_T)} \qquad (1)$$

Email address: sergio.pereira@lnf.infn.it (Sergio Anefalos Pereira)

where $f \sim 0.14$ (dependent on kinematics) is the dilution factor, $y = \nu/E$, and $N^{\pm}$ are luminosity-weighted counts for anti-parallel and parallel electron and proton helicities. The contribution from the longitudinal photon is accounted for in the depolarization factor $D'(y)$. The average beam and target polarizations are $P_b \sim 70\%$ and $P_t \sim 75\%$, respectively.

The double-spin asymmetry results for π^+ (left), π^- (center) and π^0 (right) are shown in Fig. 1 as a function of P_T, integrated over all other variables [2]. The P_T-dependence of the double-spin asymmetry can be related to the transverse momentum distributions of quarks [3] that is different for quarks polarized in the direction of the proton spin and opposite to it [4, 5]. In Fig. 1 the measured A_1 is compared to calculations of the Torino group [3], which uses different values of the ratio of widths in k_T for partonic helicity g_1 and momentum f_1 distributions, assuming Gaussian k_T distributions [2].

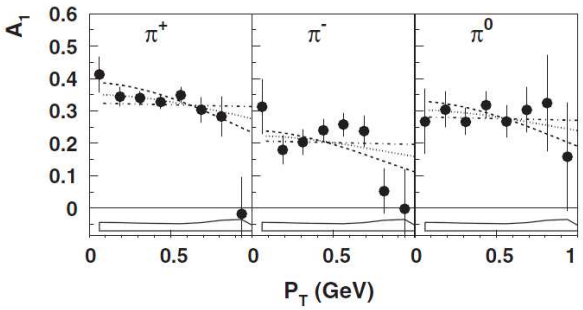

Figure 1: The double-spin asymmetry A_1 as a function of transverse momentum P_T, integrated over all other kinematical variables. The open band corresponds to systematic uncertainties. The dashed, dotted, and dash-dotted curves are calculations for different values for the ratio of transverse momentum widths for g_1 and f_1 (0.40, 0.68, 1.0) for a fixed width for f_1 (0.25 GeV^2) [2].

In Fig. 2 preliminary double-spin asymmetry results from the *eg1-dvcs* experiment [6] for π^+ (red symbols), π^- (blue symbols) and π^0 (green symbols) as a function of P_T, integrated over all other variables are shown [7]. Overall, the results are compatible with the published ones.

The double-spin asymmetry as a function of Bjorken x for π^+ (filled-up triangles), π^- (filled-down triangles) and π^0 (filled-circles) from CLAS, integrated over all other variables, is shown in Fig. 3 [8]. Also in Fig. 3 HERMES [9] results for π^+ (open-up triangles) are shown.

In Fig. 4 preliminary double-spin asymmetry results from *eg1-dvcs* for π^+ (red symbols), π^- (blue symbols) and π^0 (green symbols) as a function of P_T for six different Bjorkin x bins, integrated over all other variables are shown [7]. Overall, the current results are compatible with the published ones.

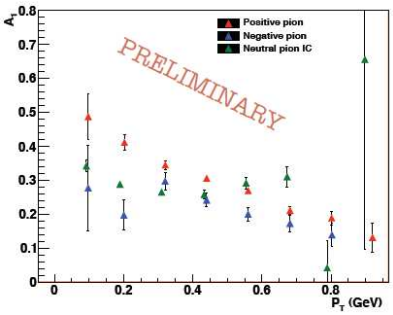

Figure 2: Preliminary double-spin asymmetry A_1 results from *eg1-dvcs* for π^+ (red symbols), π^- (blue symbols) and π^0 (green symbols) as a function of transverse momentum P_T, integrated over all other kinematical variables [7].

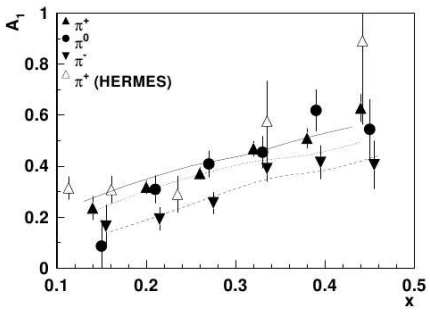

Figure 3: The double-spin asymmetry as a function of x from a polarized proton target for different π^+, π^-, and π^0 [8]. Open triangles correspond to the HERMES measurement of A_1 for π^+ [9]. Only statistical uncertainties are shown. The solid, dashed and dotted curves, calculated using LO GRSV PDF [10] and $D_1^{d\to\pi+}/D_1^{u\to\pi+}$ [11], correspond to π^+, π^-, and π^0, respectively.

3.2. *Target Single-Spin Asymmetry*

The longitudinally polarized (L) target spin asymmetry for an unpolarized beam (U), A_{UL}, is defined as

$$A_{UL} = \frac{1}{f P_t} \frac{N^+ - N^-}{N^+ + N^-} \qquad (2)$$

where $f \sim 0.14$ is the dilution factor, P_t is the average target polarization (~75%) and $N^{\pm}$ are luminosity-weighted counts for anti-parallel and parallel electron and proton helicities.

The $\sin 2\phi$ moment $A_{UL}^{sin2\phi}$ as a function of x is plotted in Fig. 5 [2]. Calculations [12, 13] using $h_{1L}^{\perp}$ from

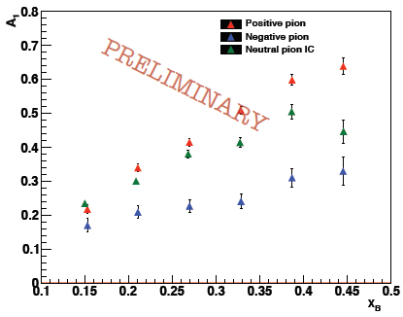

Figure 4: Preliminary double-spin asymmetry A_1 from *eg1-dvcs* as a function of P_T for six different Bjorken x bins, integrated over all kinematical variables [7].

the chiral quark soliton model [14] and the Collins function [15] extracted from HERMES [16] and Belle [17] data, are plotted as filled bands in Fig. 5. The kinematic dependence of the SSA for π^+ from the CLAS data is roughly consistent with these predictions.

The interpretation of the π^- data, which tend to have SSAs with a sign opposite to expectations, may require accounting for additional contributions (e.g., interference effects from exclusive $\rho^0 p$ and $\pi^-\Delta^{++}$ channels). This will require a detailed study with higher statistics of both double and single spin asymmetries for pions coming from decays.

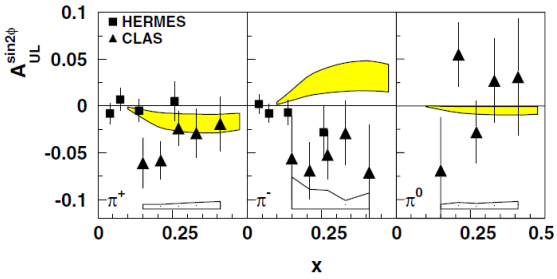

Figure 5: The measured x dependence of the longitudinal target SSA $A_{UL}^{sin2\phi}$ (triangles). The squares show the existing measurement of $A_{UL}^{sin2\phi}$ from HERMES. The lower band shows the systematic uncertainty. The upper band shows the existing theory predictions with uncertainties due to the Collins function [12, 15].

In Fig. 6 preliminary longitudinal target SSA $A_{UL}^{sin2\phi}$ results from *eg1-dvcs* for π^+ (red symbols), π^- (blue symbols) and π^0 (green symbols) as a function of x are shown [7]. The high statistics of the new data allows bi-dimensional binning for a more complete analysis.

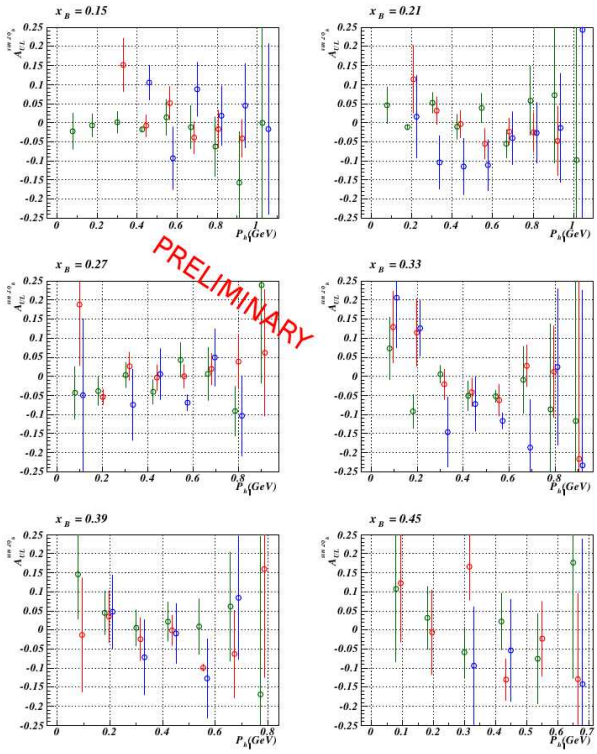

Figure 6: Preliminary $\sin 2\phi$ moments of A_{UL} as a function of P_T for different bins in x from *eg1-dvcs*. The average value of x is displayed in the title of each plot for π^+ (red), π^- (blue) and π^0 (green) [7].

3.3. Di-Hadron Beam Spin Asymmetry

Pairs of hadrons detected in the current-fragmentation region allow us to study higher-twist distribution functions, which describe quark-gluon correlations. The chiral-odd Di-Hadron Fragmentation Functions (DiFF) describe correlations between the transverse polarization of the fragmenting quark and the azimuthal orientation of the plane containing the detected hadron pair. Kinematical dependencies of the $\sin\phi$ moments can be used to probe the underlying distributions and fragmentation functions. Following the Trento conventions [18], all relevant angles are defined in Fig. 7.

The longitudinally polarized (L) beam spin asymmetry for an unpolarized target (U), A_{LU}, is defined as

$$A_{LU} = \frac{1}{P_B}\frac{N^+ - N^-}{N^+ + N^-} \qquad (3)$$

where $P_B \sim 0.85$ is the average beam polarization.

In Fig. 8 preliminary beam spin asymmetries results from *eg1-dvcs* for $\pi^+\pi^-$ pairs as a function of ϕ_R, integrated over all other kinematical variables, are shown.

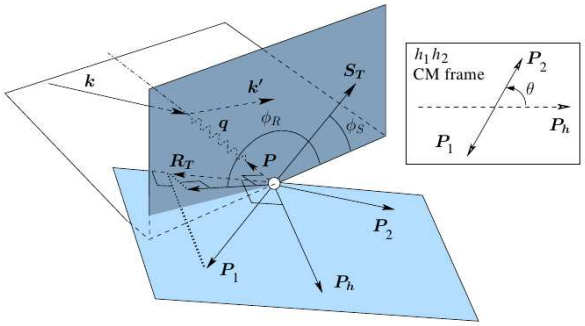

Figure 7: Depiction of the azimuthal angles ϕ_R of the dihadron and ϕ_S of the transverse target spin component S_T which is transverse to both the virtual-photon and target-nucleon momenta q and P. Both angles are evaluated in the virtual-photon-nucleon center-of-momentum frame. Explicitly, $\phi_R \equiv \frac{(q\times k)\cdot R_T}{|(q\times k)\cdot R_T|} \arccos \frac{(q\times k)\cdot(q\times R_T)}{|q\times k||q\times R_T|}$ and $\phi_S \equiv \frac{(q\times k)\cdot S_T}{|(q\times k)\cdot S_T|} \arccos \frac{(q\times k)\cdot(q\times S_T)}{|q\times k||q\times S_T|}$. Here, $R_T = R - (R\cdot\hat{P}_h)\hat{P}_h$, with $R \equiv (P_1 - P_2)/2, P_h \equiv P_1 + P_2$, and $\hat{P}_h \equiv P_h/|P_h|$, thus R_T is the component of P_1 orthogonal to P_h, and $\phi_{R\perp}$ is the azimuthal angle of R_T about the virtual-photon direction. The dotted lines indicate how vectors are projected onto planes. The short dotted line is parallel to the direction of the virtual photon. Also included is a description of the polar angle θ, which is defined as the angle between the direction of P_1 in the hadron pair center-of-mass frame, and the direction of P_h in the photon-target rest frame.

Although one expects only a $\sin(\phi_R)$ component, the distribution was fitted using $p_0 sin(\phi_R) + p_1 sin(2\phi_R)$ function. A non zero $\sin(\phi_R)$ amplitude has been observed as well as a non zero $\sin(2\phi_R)$ (the last most probably comes from acceptance effects).

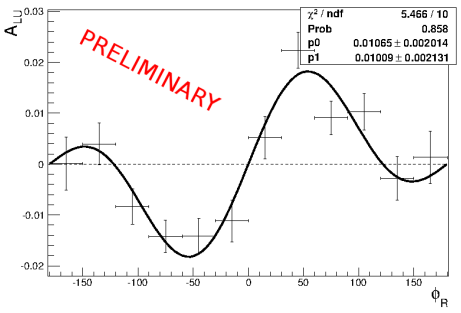

Figure 8: Preliminary beam spin asymmetries results from *eg1-dvcs* for $\pi^+\pi^-$ pairs as a function of ϕ_R, integrated over all other kinematical variables. The distribution was fitted using $p_0 \sin(\phi_R) + p_1 \sin(2\phi_R)$ function.

4. Conclusions

TMDs are needed to understand the inner structure of the nucleon, including the origin of nucleon spin. The study of TMDs is one of the main items in the JLab physics program already started. The 6 GeV experiments at JLab have shown evidence of sizable effects due to TMDs. New 12 GeV experiments are in preparation at JLab, with higher luminosity and improved detectors, to test fundamental properties of TMDs. These will allow azimuthal moment extraction in a multidimensional analysis with high statistics.

References

[1] B. A. Mecking *et al.*, Nucl. Instrum. Methods A **503**, 444 (2003).
[2] H. Avakian *et al.* Phys. Rev. Let **105**, 262002 (2010).
[3] M. Anselmino *et al.* Phys. Rev. D **74**, 074015 (2006).
[4] S. J. Brodsky *et al.* Nucl. Phys. B **441**, 197 (1995).
[5] H. Avakian *et al.* Phys. Rev. Lett. **99**, 082001 (2007).
[6] H. Avakian, http://clasweb.jlab.org/shift/eg1-dvcs/PR05-113.pdf
[7] S. Jawalkar, PhD thesis http://www.jlab.org/Hall-B/general/thesis/Jawalkar_thesis.pdf (2012).
[8] H. Avakian, http://arxiv.org/abs/arXiv:1003.4549 (2010).
[9] A. Airapetian *et al.* Phys. Rev. D**71**, 012003 (2005).
[10] M. Gluck *et al.* Phys. Rev. D**53**, 4775 (1996).
[11] A. Kotzinian Nucl. Phys. B**441**, 234 (1995).
[12] H. Avakian *et al.* Phys. Rev. D **77**, 014023 (2008).
[13] A. V. Efremov *et al.* Phys. Rev. D **67**, 114014 (2003).
[14] P. Schweitzer *et al.* Phys. Rev. D **64**, 034013 (2001).
[15] A. V. Efremov *et al.* Phys. Rev. D **73**, 094025 (2006).
[16] A. Airapetian *et al.* Phys. Rev. Lett. **94**, 012002 (2005).
[17] K. Abe *et al.* Phys. Rev. Lett. **96**, 232002 (2006).
[18] A. Bacchetta *et al.* Phys. Rev. D **70** 117504 (2004).